10 Linear control structure for wind power plants with DFIM

Due to the mechanical wear at the slip-rings wound rotor induction machines are only rarely used as motors today. Regardless, they gain increasing importance for generator applications in wind and water power plants. Their main advantage in this area is that the inverter in the rotor circuit can be designed to a smaller capacity with regard to the maximum generator output. Furthermore, the DFIM can be ran in a comparatively large slip range which allows for better utilization of the available wind energy.

10.1 Construction of wind power plants with DFIM

By means of a bidirectional converter in the rotor circuit the DFIM is able to work as a generator in both subsynchronous and oversynchronous operating areas. In both cases the stator is feeding energy into the mains. Figures 10.1b and 10.1c show the energy flow in both operating areas. The rotor:

- takes energy from the mains in subsynchronous mode and
- feeds energy back to the mains in oversynchronous mode.

Independent of the mechanical speed (subsynchronous, oversynchronous) only the sign of the electrical torque determines if the DFIM is working in motor or in generator mode. According to figure 10.1a the generator mode is defined by a negative torque. The torque amplitude is equivalent to the delivered or received active power of the machine. During dynamic changes of torque or active power the adjusted power factor of the plant is required to stay uninfluenced and constant.

The front-end converter controls the active power flow into the DC link by controlling the DC link voltage amplitude. The inverter on the rotor side (figures 1.9, 1.10) is responsible for the adjustment of the desired torque. The control strategy for the reactive current in both inverters is designed to establish the desired power factor of the overall plant.

Therefore the generator is capable to work as reactive power compensator or reactive power generator as well.

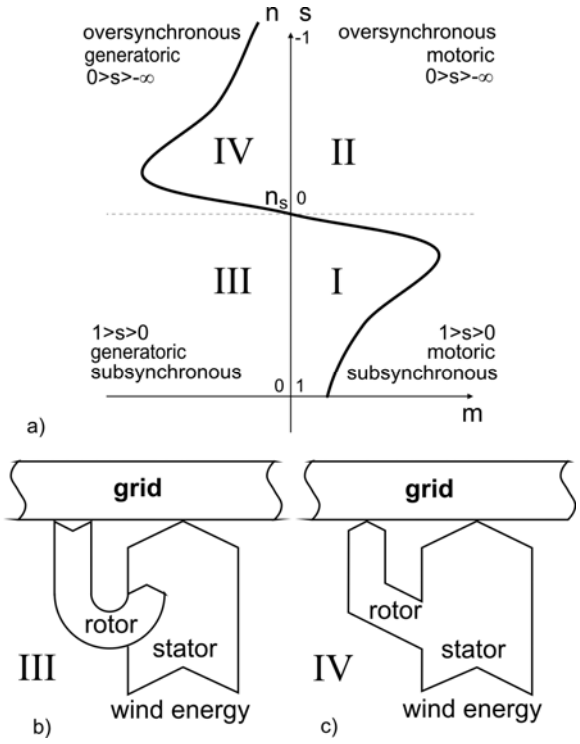

Fig. 10.1 Operating areas of the DFIM and energy flow in generator: (**a**) Operating areas of the DFIM; (**b**) Energy flow in subsynchronous mode; (**c**) Energy flow in oversynchronous mode

A number of works have been published in the recent years dealing with the problem of variable speed generators in wind or water power applications ([Suchaneck 1985], [E-Cathor 1987], [Dietrich 1990], [Pena 1995], [Tnani 1995], [Stemmler 1995]). Some of them are investigating different configurations for the converter-generator system like synchronous generator [E-Cathor 1987], oversynchronous cascade converter with natural commutation [Dietrich 1990]. In [Suchaneck 1985] a DFIM generator system for the small power range is proposed using the rotor current components as actuating variables for active and reactive power. A decoupled control of torque and rotor excitation current is presented in [Pena 1995] using stator flux orientation. Special attention is given to optimum speed tracking of the wind turbine. In [Tnani 1995] a decoupled control of active and reactive power is developed using a

complete dynamic machine model for decoupling. A predictive load model is introduced to consider changing consumer conditions on the grid.

The chapter 10 deals with the often and successfully practiced control concept with decoupling between the torque m_G and the power factor cosφ, and therewith between the active power P and reactive power Q [Quang 1997]. The design of the system is shown in the figure 10.2.

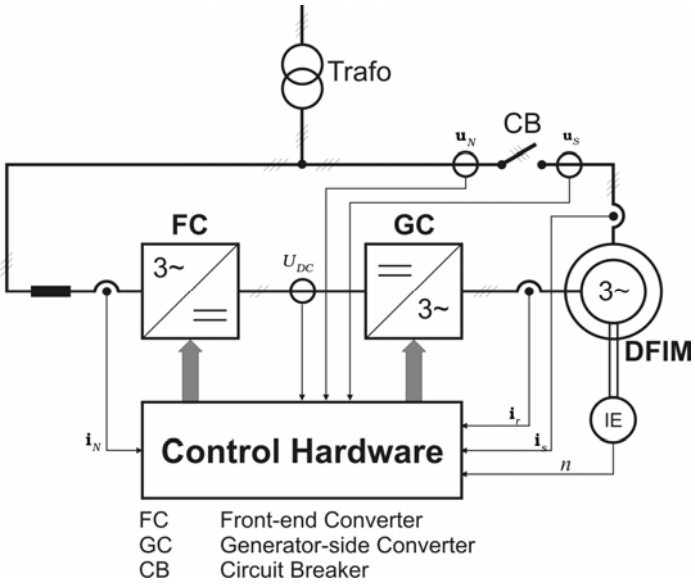

Fig. 10.2 Construction of the wind power plants using DFIM

10.2 Grid voltage orientated controlled systems

The equations (1.9) – (1.15) and the representations in the section 1.3 have indicated the meaning of the grid voltage orientation in short form. The stator of the machine is connected to the constant-voltage constant-frequency mains system. Since the stator frequency is always identical to the mains frequency, the voltage drop across the stator resistance can be neglected compared to the voltage drop across the main and leakage inductances L_m and $L_{\sigma S}$. Therewith the equation (1.10) was obtained:

$$\mathbf{u}_s = R_s \mathbf{i}_s + \frac{d\psi_s}{dt} \quad \Rightarrow \quad \mathbf{u}_s \approx \frac{d\psi_s}{dt} \text{ or } \mathbf{u}_s \approx j\omega_s \psi_s \tag{10.1}$$

Equations (10.1) say that the stator flux is always lagging the stator voltage by a phase angle of nearly 90 degree. Therefore the orientation of

the reference frame to the stator voltage approximately means orientation to the stator flux as well.

- For stator flux orientation: $u_{sd} = 0$, $\psi_{sq} = 0$
- For grid voltage orientation: $u_{sq} = 0$, $\psi_{sd} = 0$

The implementation of the grid voltage orientation requires the accurate and robust acquisition of the phase angle of the grid voltage fundamental wave, considering strong distortions due to converter mains pollution or other harmonic sources. Usually this is accomplished by means of a phase locked loop (PLL).

10.2.1 Control variables for active and reactive power

The torque of the DFIM is defined as:

$$m_G = \frac{3}{2} z_p \left(\boldsymbol{\psi}_s \times \mathbf{i}_s \right) = -\frac{3}{2} z_p \left(\boldsymbol{\psi}_r \times \mathbf{i}_r \right) \tag{10.2}$$

The equation (10.2) opens several ways for calculating the electrical torque m_G. Because the DFIM is controlled from the rotor circuit, the design of the torque control requires a form of the torque equation which includes the rotor current. After introducing the rotor current into the first part of (10.2) the following formula will be obtained:

$$m_G = -\frac{3}{2} z_p \frac{L_m}{L_s} \left(\boldsymbol{\psi}_s \times \mathbf{i}_r \right) = -\frac{3}{2} z_p \left(1-\sigma\right) L_r \left(\boldsymbol{\psi}_s^{/} \times \mathbf{i}_r \right) \tag{10.3}$$

Considering the grid voltage reference frame (reference coordinate system) with $\psi_{sd} = 0$, equation (10.3) can be simplified to:

$$m_G = -\frac{3}{2} z_p \frac{L_m}{L_s} \psi_{sq} i_{rd} = -\frac{3}{2} z_p \left(1-\sigma\right) L_r \psi_{sq}^{/} i_{rd} \tag{10.4}$$

Because the stator flux is kept constant by the constant grid voltage (refer to (10.1)) *the component i_{rd} may be considered as the torque forming current which also represents the active power P of the generator*.

The equation (10.4) needs the knowledge of the machine inductances for the torque calculation. The main inductance depends on the magnetization working point which is determined by the grid voltage amplitude. For the latter tolerances of at least +/-10% must be considered because the working point may be shifted into or out of the saturation range due to variations of the grid voltage amplitude. Therefore, using equation (1.16) for torque feedback calculation requires an accurate measuring and consideration of the L_m saturation characteristic, otherwise the requirements for the torque accuracy cannot be fulfilled. It would be

better to utilize a torque model which does not require the knowledge of any machine parameters, or at least not any working point dependent ones like the main inductance. For this, the left equation (10.2) offers itself. Substituting the stator flux linkage by the first equation of (3.77) and considering grid voltage orientation with $d\psi_s/dt = 0$ it is obtained:

$$m_G = \frac{3}{2} z_p \frac{u_{sd} i_{sd} - R_s i_s^2}{\omega_s} \tag{10.5}$$

For usual values of the stator resistance of large machines, (10.5) can be re-written with good approximation to:

$$m_G = \frac{3}{2} z_p \frac{u_{sd} i_{sd}}{\omega_s} \tag{10.6}$$

On the other hand it was already shown in the section 1.3 that thanks to the relations (1.12), (1.14) and (1.15) *the current i_{rq} is regarded as a cosφ forming component or as the decisive current for the reactive power Q.*

10.2.2 Dynamic rotor current control for decoupling of active and reactive power

The control system of the DFIM consists of two parts: the generator-side control and the grid-side control (front-end converter control), in which the generator-side control was already introduced in the figure 1.9.

In section 3.4 the (continuous and discrete) state space models of the DFIM were introduced. Since the two rotor current components i_{rd}, i_{rq} play the role of *P* and *Q* control variables an inner control loop to impress the rotor current is needed.

The process model of the rotor current is represented by the figure 3.15b and by the first of both equations (3.85):

$$\mathbf{i}_r(k+1) = \mathbf{\Phi}_{11}\mathbf{i}_r(k) + \mathbf{\Phi}_{12}\boldsymbol{\psi}_s'(k) + \mathbf{H}_{s1}\mathbf{u}_s(k) + \mathbf{H}_{r1}\mathbf{u}_r(k) \tag{10.7}$$

After splitting (10.7) into its real and imaginary components, the following equations are obtained in the grid voltage orientated reference frame:

$$\begin{cases} i_{rd}(k+1) = \Phi_{11} i_{rd}(k) + \Phi_{12} i_{rq}(k) + \Phi_{14}\psi_{sq}'(k) \\ \qquad\qquad + h_{11s} u_{sd}(k) + h_{11r} u_{rd}(k) \\ i_{rq}(k+1) = -\Phi_{12} i_{rd}(k) + \Phi_{11} i_{rq}(k) + \Phi_{13}\psi_{sq}'(k) \\ \qquad\qquad + h_{11r} u_{rq}(k) \end{cases} \tag{10.8}$$

In (10.8) the stator flux and the stator voltage might be regarded as disturbances to be compensated by a feed-forward control. These values are nearly constant and therefore can be compensated exactly and fast enough by the implicit integral part of the controller, so that their feed-forward compensation may be omitted. Regardless, the compensation shall be included in the following steps to achieve a more coherent design.

The further design is identical to the description in the chapter 5. Introducing $\mathbf{y}(k)$ as output value of the vector controller $\mathbf{R}_i$, the following approach for the feed-forward compensation network may be constructed:

$$\mathbf{u}_r(k+1) = \mathbf{H}_{r1}^{-1}\left[\mathbf{y}(k) - \boldsymbol{\Phi}_{12}\psi_s'(k+1) - \mathbf{H}_{s1}\mathbf{u}_s(k+1)\right] \tag{10.9}$$

After inserting (10.9) into (10.7) the compensated process will be obtained:

$$\mathbf{i}_r(k+1) = \boldsymbol{\Phi}_{11}\mathbf{i}_r(k) + \mathbf{y}(k-1) \text{ or } z\,\mathbf{i}_r(z) = \boldsymbol{\Phi}_{11}\mathbf{i}_r(z) + z^{-1}\mathbf{y}(z) \tag{10.10}$$

The structure of the current controller is shown in the figure 10.3. The compensated process equation (10.10) contains a dead time of one sampling interval $\mathbf{y}(k\text{-}1)$ to account for the delay between the feedback acquisition and the voltage output (computing delay). $\mathbf{y}(k\text{-}1)$ fulfills the following equation in the z-domain:

$$\mathbf{y}(z) = \mathbf{R}_I\left[\mathbf{i}_r^*(z) - \mathbf{i}_r(z)\right] \tag{10.11}$$

Superscript „*“: reference value (set point)

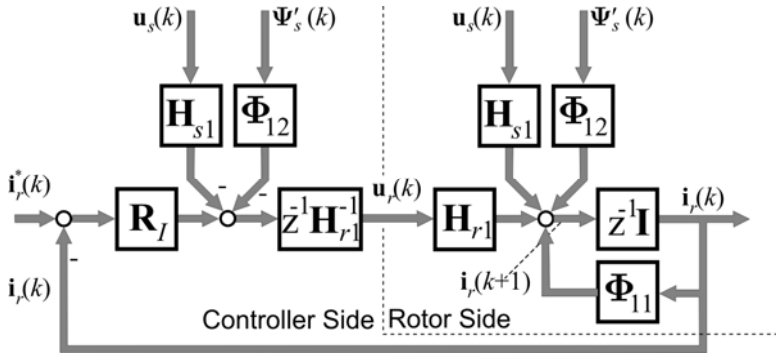

Fig. 10.3 Rotor current control structure using feed-forward compensation of stator voltage and stator flux

After substituting (10.11) into (10.10) the following transfer function of the closed current loop will be obtained:

$$\mathbf{i}_r(z) = z^{-1}\left[z\mathbf{I} - \boldsymbol{\Phi}_{11} + z^{-1}\mathbf{R}_I\right]^{-1}\mathbf{R}_I\mathbf{i}_r^*(z) \tag{10.12}$$

Similarly to the chapter 5 a vector controller with dead-beat behavior for (10.12) is given by:

$$\mathbf{R}_I = \frac{\mathbf{I} - z^{-1}\mathbf{\Phi}_{11}}{1 - z^{-2}} \tag{10.13}$$

The dead-beat behavior results in fast dynamics and accuracy, the vector design ensures good decoupling between the components i_{rd} and i_{rq}. For a less fast (and thus less noise sensitive) behavior, designs with finite adjustment times (cf. section 5.3.3) or PI-type designs may be applicable as well.

If the tracking errors are defined as:

$$x_{wd}(k) = i_{rd}^{*}(k) - i_{rd}(k);\ x_{wq}(k) = i_{rq}^{*}(k) - i_{rq}(k) \tag{10.14}$$

the controller equations in the time-domain including the disturbance feed-forward compensation can be written as follows:

$$\begin{cases} u_{rd}(k+1) = h_{11r}^{-1}\left[x_{wd}(k) - \Phi_{11}x_{wd}(k-1) - \Phi_{12}x_{wq}(k-1) \right. \\ \qquad\qquad \left. + y_d(k-2) - \Phi_{14}\psi_{sq}^{/} - h_{11s}u_{sd}\right] \\ u_{rq}(k+1) = h_{11r}^{-1}\left[x_{wq}(k) + \Phi_{12}x_{wd}(k-1) - \Phi_{11}x_{wq}(k-1) \right. \\ \qquad\qquad \left. + y_q(k-2) - \Phi_{13}\psi_{sq}^{/}\right] \end{cases} \tag{10.15}$$

The complete structure of the generator-side control was already shown in the figure 1.9.

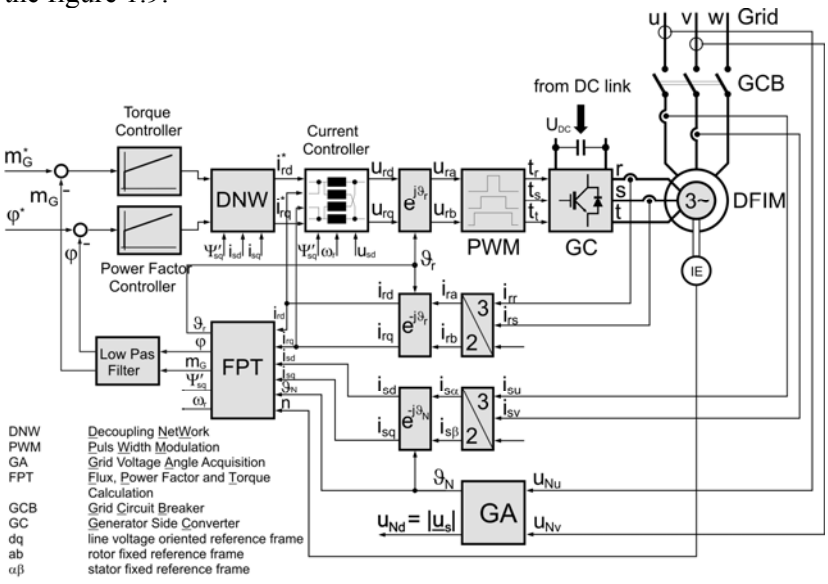

Fig. 10.4 Generator-side control structure using linear rotor current controller

10.2.3 Problems of the implementation

The decoupling structure in the figure 10.4 consists of two essential functional blocks:

- Calculation of the feedback (actual) values for torque and power factor using stator voltage, currents and speed (block FPT) and
- Calculation of the current set points (block DNW).

a) Block FPT: The following equations are realized:

- Calculation of stator flux:

$$\psi'_{sq} \approx i_{sq} + i_{rq} \tag{10.16}$$

- Calculation of torque:

$$m_G = \frac{3}{2} z_p \frac{u_{sd} i_{sd}}{\omega_s} \tag{10.17}$$

- Calculation of stator current amplitude:

$$|\mathbf{i}_s| = \sqrt{i_{sd}^2 + i_{sq}^2} \tag{10.18}$$

- Calculation of sinφ:

$$\sin\varphi = \frac{i_{sq}}{|\mathbf{i}_s|} \tag{10.19}$$

The calculated torque and sinφ values are serving as feedbacks for the torque and power factor control. Both controllers are of PI type.

b) Block DNW: Using the torque and power factor controller outputs y_M and y_φ, the reference values for the inner-loop current control are calculated as follows:

- Torque forming current component i_{rd}^*:

$$i_{rd}^* = \frac{y_M}{-\frac{3}{2} z_p (1-\sigma) L_r \psi'_{sq}} \tag{10.20}$$

- sinφ forming current component i_{rq}^*:

$$i_{rq}^* = \psi'_{sq} - y_\varphi |\mathbf{i}_s| \tag{10.21}$$

The effectiveness of the decoupling is shown in figure 10.5. The diagrams show step responses of the torque and the power factor at both oversynchronous and subsynchronous speed. For the subsynchronous case both low pass filtered and unfiltered values of the torque and power factor

are depicted. The control is optimized to the filtered values therefore the unfiltered values exhibit a stronger overshot. As already pointed out a nearly undelayed injection of the reference values is theoretically possible, however, measurement noise and current harmonics force to slow down the control dynamics. The adjusted rise time of the unfiltered torque of about 30 ms fulfills all practical requirements. During the torque transients (step size about half the nominal torque) almost no changes of cosφ are visible, the same applies for the torque during cosφ transients.

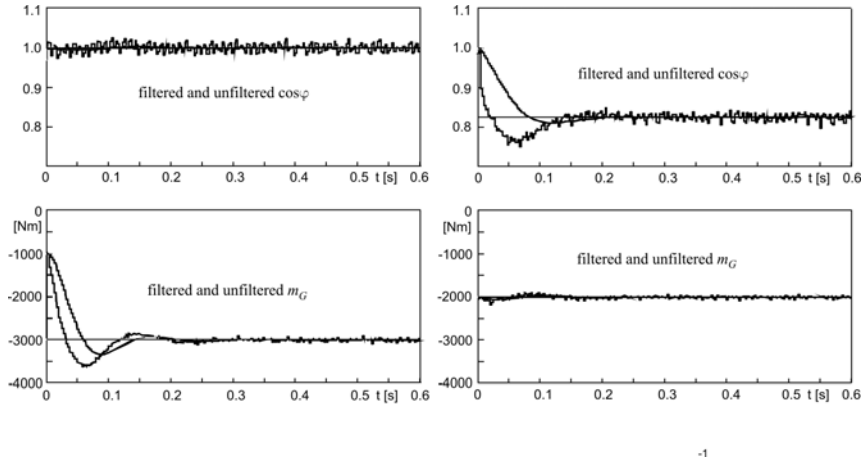

Fig. 10.5 Torque and cosφ step changes of a 620kW generator. (**left**) Torque reference -1000 → -3000Nm; (**right**) cosφ reference 1.0 → 0.825

10.3 Front-end converter current control

The front-end converter control is feeding the DC link from the grid during subsynchronous operation and feeds back energy to the supply during oversynchronous operation. This task is accomplished by means of a DC link voltage control, which is supposed to keep a constant bus voltage in all operation modes. Corresponding to the generator control the grid side contains a power factor control loop which compensates the line filter reactive-power demand and in connection with the generator-side realizes the reactive power reference for the overall plant.

The output current of the mains converter $\mathbf{i}_N$ can be split as usual into real and imaginary parts:

$$\mathbf{i}_N = i_{Nd} + j\, i_{Nq} \tag{10.22}$$

In the grid voltage orientated reference frame, the real part acts as active power producing component and the imaginary part as reactive power producing component. Therefore, i_{Nd} is a good choice to be used as control variable for the DC link voltage. Appropriately, i_{Nq} forms the control variable for the power factor control on the grid side. Similarly to the generator control, the power factor is controlled indirectly via $\sin\varphi$, being direct proportional to i_{Nq}, cf. equation (1.15). Both U_{DC} and $\sin\varphi$ controllers are of PI-type.

The commands i_{Nd} and i_{Nq} are realized by an inner-loop current control. Therefore the complete structure of the grid-side control can be given like in the figure 1.10.

As it had turned out in the previous section, the current control plays a decisive role in the control concept and for its correct realization. Therefore it shall be described in some more detail in the following section. All current control loops are designed in the grid voltage orientated reference frame.

10.3.1 Process model

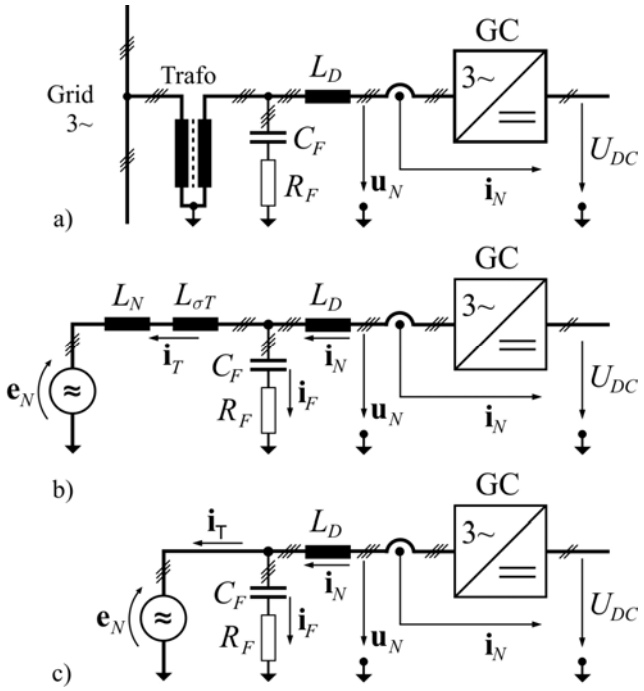

Fig. 10.6 Grid-side control plant: (**a**) Common grid-side scheme; (**b**) Equivalent circuit; (**c**) Equivalent circuit for process model derivation

The front-end converter is usually connected to the supply through the reactor L_D, RC-filter and transformer (figure 10.6a). Considering the grid inductance L_N and at the same time replacing the transformer by its leakage inductance $L_{\sigma T}$ and the grid by the voltage source $\mathbf{e}_N$ gives the equivalent circuit in the figure 10.6b. The voltage drop over the transformer and the grid inductance is considerably smaller then the one over the RC-filter and therefore may be neglected. Taking into account the resistance R_D of the inductor the equivalent circuit in figure 10.6c is finally obtained as the starting-point for the derivation of the current control process model (R_D is not drawn here).

In steady state condition the following filter equation is derived from figure 10.6c:

$$\mathbf{e}_N = \frac{1}{j\omega_s C_F}\mathbf{i}_F + R_F\mathbf{i}_F \tag{10.23}$$

In the grid voltage orientated reference frame and with:

$$\mathbf{e}_N = e_{Nd} + je_{Nq};\ e_{Nq} = 0 \tag{10.24}$$

equation (10.23) can be written in component form as follows:

$$\begin{cases} e_{Nd} = R_F i_{Fd} - \dfrac{1}{\omega_s C_F} i_{Fq} \\ 0 = R_F i_{Fq} + \dfrac{1}{\omega_s C_F} i_{Fd} \end{cases} \quad \text{with} \quad \mathbf{i}_F = i_{Fd} + ji_{Fq} \tag{10.25}$$

With equation (10.25) the filter currents i_{Fd} and i_{Fq} can be calculated for the stationary condition. In steady state, these currents and the grid voltage $\mathbf{e}_N$ may be considered as constant and therefore act as constant disturbances for the control loop. They may be compensated by feed-forward control or by an integral part in the controller.

The grid current and voltage equations can be derived from the figure 10.5c:

$$\begin{cases} \mathbf{u}_N = R_D\mathbf{i}_N + L_D\dfrac{d\mathbf{i}_N}{dt} + \mathbf{e}_N \\ \mathbf{i}_N = \mathbf{i}_T + \mathbf{i}_F \end{cases} \tag{10.26}$$

After transforming (10.26) into the grid voltage orientated reference frame and substituting the current $\mathbf{i}_N$ from the first equation of (10.26) by the second equation the new voltage equation is obtained:

$$\mathbf{u}_N = R_D\mathbf{i}_T + L_D\frac{d\mathbf{i}_T}{dt} + j\omega_s L_D\mathbf{i}_T + \mathbf{e}_{Nv} \tag{10.27}$$

with:

$$\begin{aligned}&\mathbf{e}_{Nv} = \mathbf{e}_N + j\omega_s L_D \mathbf{i}_F + R_D \mathbf{i}_F = e_{Nvd} + je_{Nvq}\\ &L_D \frac{d\mathbf{i}_F}{dt} = 0\end{aligned} \tag{10.28}$$

From (10.27) the continuous process model in the state space can be written in component form:

$$\begin{cases}\dfrac{di_{Td}}{dt} = -\dfrac{1}{T_D} i_{Td} + \omega_s i_{Tq} + \dfrac{1}{L_D}\left(u_{Nd} - e_{Nvd}\right)\\ \dfrac{di_{Tq}}{dt} = -\omega_s i_{Td} - \dfrac{1}{T_D} i_{Tq} + \dfrac{1}{L_D}\left(u_{Nq} - e_{Nvq}\right)\end{cases} \tag{10.29}$$

The time discrete state space model is given immediately by:

$$\mathbf{i}_T(k+1) = \mathbf{\Phi}_N \mathbf{i}_T(k) + \mathbf{H}_N \mathbf{u}_N(k) - \mathbf{H}_N \mathbf{e}_{Nv}(k) \tag{10.30}$$

with:

$$\mathbf{\Phi}_N = \begin{bmatrix} 1 - \dfrac{T}{T_D} & \omega_s T \\ -\omega_s T & 1 - \dfrac{T}{T_D} \end{bmatrix};\ \mathbf{H}_N = \begin{bmatrix} \dfrac{T}{L_D} & 0 \\ 0 & \dfrac{T}{L_D} \end{bmatrix} \tag{10.31}$$

With the process model (10.30) the controller design can be carried out now. If only the inverter output current $\mathbf{i}_N$ is measured, the filter current $\mathbf{i}_F$ must be calculated by means of (10.25) and finally the grid (or transformer) current $\mathbf{i}_T$ using (10.26).

10.3.2 Controller design

The design is similar to the rotor current controller. With the controller output $\mathbf{y}_N(k)$, the following equation can be written for the feed-forward compensation network according to (10.30) considering the computation time delay:

$$\mathbf{u}_N(k+1) = \mathbf{H}_N^{-1}\left[\mathbf{y}_N(k) + \mathbf{H}_N \mathbf{e}_{Nv}(k+1)\right] \tag{10.32}$$

After substituting (10.32) into (10.31) the compensated process model is given:

$$\mathbf{i}_T(k+1) = \mathbf{\Phi}_N \mathbf{i}_T(k) + \mathbf{y}_N(k-1) \tag{10.33}$$

Two things have to be mentioned here:

- The structure of the compensated process model is totally identical with the one of the rotor side (10.10).
- Likewise, $\mathbf{e}_N(k)$ acts as constant disturbance and therefore may be compensated automatically by an implicit integral part in the controller without any special compensation.

For control with dead-beat response and a good decoupling between the current components the controller equation can be immediately written to:

$$\mathbf{R}_{IN} = \frac{\mathbf{I} - z^{-1}\mathbf{\Phi}_N}{1 - z^{-2}} \tag{10.34}$$

Neglecting the feed-forward compensation of the constant disturbances the equation of the controller is obtained in the time domain as:

$$\begin{cases} u_{Nd}(k+1) = \dfrac{L_D}{T}\left[x_{Td}(k) - \left(1 - \dfrac{T}{T_D}\right)x_{Td}(k-1) - \omega_s T x_{Tq}(k-1) \right. \\ \qquad\qquad \left. + y_{Nd}(k-2)\right] \\ u_{Nq}(k+1) = \dfrac{L_D}{T}\left[x_{Tq}(k) + \omega_s T x_{Td}(k-1) - \left(1 - \dfrac{T}{T_D}\right)x_{Tq}(k-1) \right. \\ \qquad\qquad \left. + y_{Nq}(k-2)\right] \end{cases} \tag{10.35}$$

with:

$$\mathbf{x}_T = x_{Td} + jx_{Tq}\ ;\ x_{Td} = i_{Td}^{*} - i_{Td}\ ;\ x_{Tq} = i_{Tq}^{*} - i_{Tq}\ ;\ \mathbf{y}_N = y_{Nd} + jy_{Nq}$$

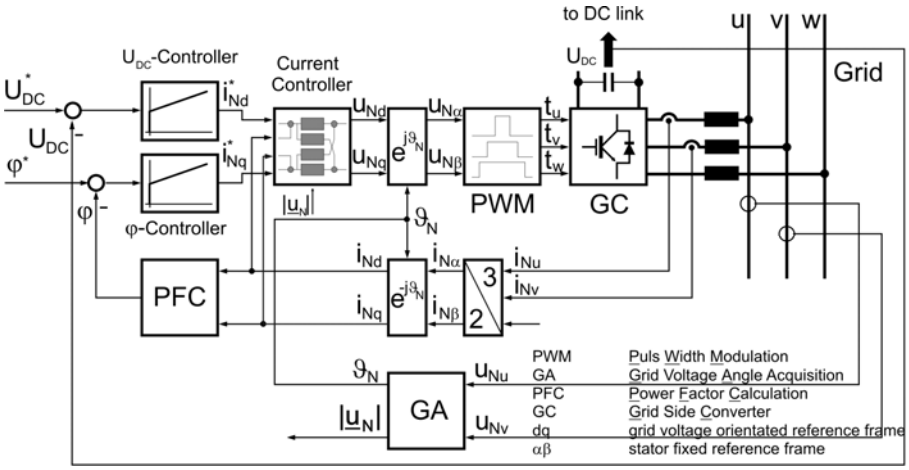

Fig. 10.7 Complete grid-side control structure

Because the control starts with immediately connected disturbance $\mathbf{e}_N$, the controller output $\mathbf{y}_N$ and its past values must be pre-initialized to avoid undesirable transients:

$$\mathbf{y}_N(k=0) = -\mathbf{H}_N \mathbf{e}_{Nv}(k=0) \tag{10.36}$$

The controller (10.34) - (10.35) works robust and reliable. However, if the reactor L_D is dimensioned too small, the high-dynamic behavior can cause undesirable ripples in the transformer or grid current $\mathbf{i}_T$. In this case a controller design with finite adjustment time would lead to a current waveform with a better THD coefficient. The complete grid-side control structure is shown in the figure 10.7 (cf. [Quang 1997]).

10.4 References to chapter 10

Arsudis D (1989) Doppeltgespeister Drehstromgenerator mit Spannungszwischenkreis-Umrichter im Rotorkreis für Windkraftanlagen. Dissertation, TU Carolo-Wilhelmina zu Braunschweig

Dietrich W (1990) Drehzahlvariables Generatorsystem für Windkraftanlagen mittlerer Leistung. Dissertation, TU Berlin

E-Cathor J (1987) Drehzahlvariable Windenergieanlage mit Gleichstromzwischenkreis-Umrichter und Optimum-suchendem Regler. Dissertation, TU Carolo-Wilhelmina zu Braunschweig

Pena RS, Clare JC, Asher GM (1995) Implementation of Vector Control Strategies for a Variable Speed Doubly-Fed Induction Machine for Wind Generator System. EPE ‘95 Sevilla, pp. 3.075 - 3.080

Quang NP, Dittrich JA (1999) Praxis der feldorientierten Drehstromantriebsregelungen. 2. Aufl., Expert-Verlag

Quang NP, Dittrich JA, Thieme A (1997) Doubly-fed induction machine as generator: control algorithms with decoupling of torque and power factor. Electrical Engineering / Archiv für Elektrotechnik, 10.1997, pp. 325-335

Späth H (1983) Steuerverfahren für Drehstrommaschinen: Theoretische Grundlagen. Springer-Verlag: Berlin Heidelberg New York Tokyo

Stemmler H, Omlin A (1995) Converter Controlled Fixed-Frequency Variable-Speed Motor/Generator. IPEC Yokohama ‘95, pp. 170 - 176

Suchaneck J (1985) Untersuchung einer doppeltgespeisten Asynchronmaschine mit feldorientierter Steuerung zur elektrischen Windenergienutzung bis 20kW. Dissertation, TU Berlin

Tnani S, Diop S, Jones SR, Berthon A (1995) Novel Control Strategy of Double-Fed Induction Machines. EPE ‘95 Sevilla, pp. 1.553 - 1.558